ORIGINAL RESEARCH

CrossMark

An NMR and DFT investigation on the interconversion of 9-substituented-N^6-hydrazone-8-azaadenine derivatives: proton migration or conformational isomerization?

Qiangwen Fan[1] · Yeming Wang[2] · Hong Yan[1]

Abstract

A newly synthesized N^6-arylhydrazone-8-azaadenine derivatives (**1**) showed significant differences in NMR spectra with previously synthesized analogues, specifically, the hydrogens of $N^{1'}H$ and $C^{3'}H$ in all the titled compounds showed two groups of signals in their ^{1}H-NMR spectra. In order to investigate whether the duplication of proton signals were related to a mixture of conformational isomers which rotated around $C-N^{1'}$ bond or configurational isomers which resulted from proton migration, variable temperature NMR and 2D-NOESY experiments were carried out in conjunction with density function theory (DFT) calculations at the B3LYP/6-311G (d,p)//B3LYP/6-31G (d,p) level. The results indicated that it was the conformational isomerism rather than hydrogen transfer that induced the reproduction of proton signals, which was attributed to lower barrier energy and larger rate constant of the former process.

Keywords N^6-hydrazone-8-azaadenine · Variable-temperature NMR · Density-functional theory (DFT) · Conformational isomerism · Proton migration

Introduction

Contrasted with natural purines, 8-azaadenines are a class of compounds characterized by the CH group of the imidazolic ring replacing by a nitrogen atom. The 8-azaadenine scaffold which served as an essentially biological activities moiety of many kinase inhibitors has attracted considerable attentions of chemists for a long time [1–8]. Some pharmaceuticals with various substituted 8-azaadenines moiety are of potent anti-thrombotic, anti-viral, and anti-neoplastic activities [9–11].

✉ Hong Yan
hongyan@bjut.edu.cn

[1] College of Life Science and Bioengineering, Beijing University of Technology, Chaoyang District, Beijing 100124, China

[2] Beijing Tide Pharmaceutical Co., Ltd, No.8 East Rongjing Street, Beijing Econnomi Technological Development Area(BDA), Beijing 100176, China

Moreover, many documents have reported that 8-azaadenines derivatives showed strong fluorescence properties and can be applied for analytical applications, for instance, using as fluorescence probe [12–14]. Besides, 8-azaadenines and their nucleosides have also been intensively studied as model systems for elucidating the mechanisms of action of natural nucleosides and their analogs in various enzyme systems [15–17]. On the other hand, it is well known that different geometric isomers of organic molecules may display distinct physical and chemical properties. In this sense, the study of conformational or configurational changes in molecules is essential in biochemistry, pharmacology, and supramolecular chemistry. Nowadays, the most popular approaches for studies of conformational interconversions are based on temperature-dependence ^{1}H NMR spectroscopy coupled with DFT calculations [18–23].

With these in mind, herein we described our studies on preparation and structural analysis of series of 8-azaadenine derivatives (Scheme 1). Interestingly, we found that the hydrogens of $N^{1'}H$ and $C^{3'}H$ in all the target compounds (**1**) showed two groups of signals in their ^{1}H-NMR spectra although this phenomenon of some compounds is less obvious at 298 K. In order to
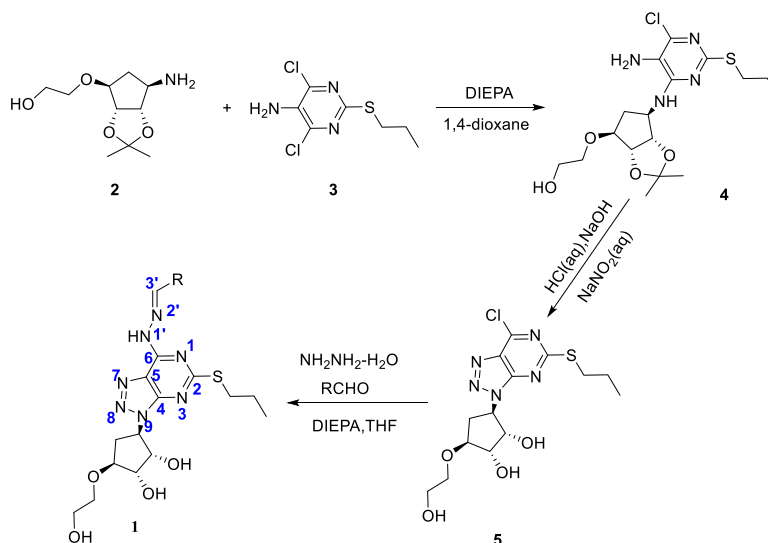
R = 3-hydroxylphenyl (**1a**); 2,4-difluorophenyl (**1b**); 4-nitrophenyl (**1c**); 4-chlorophenyl (**1d**); 3-nitrophenyl (**1e**).

investigate the source of the phenomenon, variable-temperature NMR and 2D-NOESY experiments combined with the density function theory (DFT) calculations were carried out. To best of our knowledge, it is the first description of prototropic tautomerism and conformational interconversion for 8-azaadenine derivatives from experimentally and theoretically.

Experimental methods

Physical measurements

All chemicals were purchased from commercial sources and used without further purification. Thin layer chromatography (TLC) was conducted on silica-gel 60 F254 plates (Merck KGaA). Melting points were determined on a XT-5A digital melting-point apparatus without correcting.^{1}H NMR spectra and ^{13}C NMR spectra were recorded on a Bruker Avance 400 spectrometer at 400 and 100 MHz using DMSO-d_6 as the solvent and tetramethylsilane (TMS) as the internal standard. High-resolution mass spectral (HRMS) analyses were carried out using a VG 70SE mass spectrometer from Manchester, UK, which was operated in electron impact or electrospray ionization mode.

Chemical synthesis

The titled compounds (**1**) were prepared by using compounds **2** and **3** as raw materials which underwent a nucleophilic substitution process giving rise to the intermediate **4**, followed by a diazotization and deprotection reaction to afford another intermediate **5**, which subsequently reacted with hydrazine monohydrate and aromatic aldehyde where through nucleophilic substitution and dehydration condensation reaction (Scheme 1).

General procedure for the preparation of compounds 1 A 250-ml round bottom flask was charged with solution of N,N′-diisopropylethylamine (DIEPA) (2.8 g 0.022 mol) and hydrazine monohydrate (1.1 g 0.022 mol) in 40 ml THF and stirred in ice-water bath for 30 min and then solution of **4** (8.57 g 0.022 mol) in 100 ml THF was added dropwise to the mixture and stirred until the compound **4** was no longer detectable by TLC, followed by addition of aromatic aldehyde into the reaction and stirred for 40 min when TLC showed complete disappearance of starting materials. The reaction mixture was treated with 200 ml H_2O and extracted with THF (3*20 ml). The organic layers were combined, washed with brine, dried with anhydrous Na_2SO_4, filtered, and evaporated to afford crude product and then recrystallized from THF and hexane (V/V = 3:1), resulting in pure target compounds **1**.

9-[(1′R,2′S,3′S,4′S)-2′,3′-dihydroxyl-4′-hydroxyethoxy-cyclopentane-1′-yl]-9H-2-propylthio-6-(3-hydroxylbenzaldehyde hydrazone)-8-azapurine(1a) ^{1}H NMR (400 MHz, DMSO-d_6): δ (ppm) 1.01 (3H, t, CH$_3$, J = 7.2 Hz), 1.73 (2H, m, CH$_2$), 2.07 (1H, m, CH$_2$), 2.69 (1H, m, CH$_2$), 3.14 (2H, CH$_2$), 3.51–3.53 (4H, m), 3.78 (1H, s, CH), 3.97 (1H, s, CH), 4.62 (2H, m, CH, OH), 4.99–5.18 (3H, m, CH, OH), 6.83 (1H, m, Ph-H), 7.24–7.31 (3H, Ph-H), 8.19, 8.43 (1H, =CH), 9.68 (1H, s, Ph-OH), 12.36, 12.54 (1H, NH). ^{13}C NMR (100 MHz, DMSO-d_6): δ (ppm) 13.72, 22.82, 32.72, 33.57, 60.78, 61.08, 71.26, 74.27, 74.76, 82.25, 113.32, 117.82, 119.25, 122.79, 130.25, 135.98, 146.95, 151.69, 153.54, 158.10, 168.70. HRMS (ESI) for [M + H]$^+$: calcd 490.18671, found 490.18668.

9-[(1′R,2′S,3′S,4′S)-2′,3′-dihydroxyl-4′-hydroxyethoxy-cyclopentane-1′-yl]-9H-2-propylthio-6-(3,4-diflorobenzaldehyde hydrazone)-8-azapurine(1b)

^{1}H NMR (400 MHz, DMSO-d_6): δ (ppm) 1.01 (3H, t, CH$_3$, J = 7.2 Hz), 1.73 (2H, m, CH$_2$), 2.09 (1H, m, 5′-CH$_2$), 2.67 (1H, m, 5′-CH$_2$), 3.14 (2H, CH$_2$), 3.52 (4H, m, CH$_2$), 3.78 (1H, s, CH), 3.98 (1H, s, CH), 4.63 (2H, m, CH, OH), 5.03–5.18 (3H, m, CH, OH), 7.53–7.92 (3H, m, Ph-H), 8.22, 8.46 (1H, =CH), 12.56, 12.71 (1H, NH). ^{13}C NMR (100 MHz, DMSO-d_6): δ (ppm) 13.71, 22.76, 32.73, 33.80, 60.77, 61.08, 71.28, 74.25, 74.81, 82.25, 115.40 (115.52), 118.39 (118.50), 122.86, 124.78, 132.75, 143.83, 149.36 (149.45), 150.99 (151.08), 153.67, 168.78, 170.72. HRMS (ESI) for [M + H]$^+$: calcd 510.17296, found 510.17287.

9-[(1′R,2′S,3′S,4′S)-2′,3′-dihydroxyl-4′-hydroxyethoxy-cyclopentane-1′-yl]-9H-2-propylthio-6-(4-nitrobenzaldehyde hydrazone)-8-azapurine(1c)

^{1}H NMR (400 MHz, DMSO-d_6): δ (ppm) 1.02 (3H, t, CH$_3$, J = 7.2 Hz), 1.73 (2H, m, CH$_2$), 2.11 (1H, m, 5′-CH$_2$), 2.69 (1H, m, 5′-CH$_2$), 3.16 (2H, CH$_2$), 3.35–3.53 (4H, m), 3.79 (1H, s, CH), 3.98 (1H, s, CH), 4.63 (2H, m, CH, OH), 5.04–5.18 (3H, m, CH, OH), 8.09 (2H, Ph-H), 8.30 (2H, Ph-H), 8.33, 8.60 (1H, =CH), 8.68 (1H, s, Ph-H), 12.76, 12.88 (1H, NH). ^{13}C NMR (100 MHz, DMSO-d6): δ (ppm) 13.73, 22.75, 32.79, 33.62, 60.76, 61.16, 71.27, 74.24, 74.83, 82.24, 124.52, 128.29, 141.12, 148.11. HRMS (ESI) for [M + H]$^+$: calcd 519.17688, found 519.17689.

9-[(1′R,2′S,3′S,4′S)-2′,3′-dihydroxyl-4′-hydroxyethoxy-cyclopentane-1′-yl]-9H-2-propylthio-6-(4-chlorobenzaldehyde hydrazone)-8-azapurine(1d)

^{1}H NMR (400 MHz, DMSO-d6): δ (ppm) 1.00 (3H, t, CH3, J = 7.2 Hz), 1.73 (2H, m, CH2), 2.10 (1H, m, 5′-CH2), 2.68 (1H, m, 5′-CH2), 3.14 (2H, CH2), 3.52(4H, m, CH2), 3.79 (1H, s, CH), 3.98 (1H, s, CH), 4.63 (2H, m, CH, OH), 5.03–5.18 (3H, m, CH, OH), 7.51–7.88 (4H, m, Ph-H), 8.32 8.50 (1H, =CH), 12.50, 12.64 (1H, NH). ^{13}C NMR (100 MHz, DMSO-d6): δ (ppm) 13.73, 22.79, 33.74, 33.60, 60.78, 61.08, 71.27, 74.28, 74.80, 82.26, 122.86, 129.08, 129.32, 133.75, 134.78, 145.08, 151.70, 153.61, 168.75. HRMS (ESI) for [M + H]$^+$: calcd 508.15283, found 508.15289.

9-[(1′R,2′S,3′S,4′S)-2′,3′-dihydroxyl-4′-hydroxyethoxy-cyclopentane-1′-yl]-9H-2-propylthio-6-(3-nitrobenzaldehyde hydrazone)-8-azapurine(1e)

^{1}H NMR (400 MHz, DMSO-d6): δ (ppm) 1.01 (3H, t, CH3, J = 7.2 Hz), 1.73 (2H, m, CH2), 2.14 (1H, m, 5′-CH2), 2.69 (1H, m, 5′-CH2), 3.15 (2H, CH2), 3.53 (4H, m, CH2), 3.79 (1H, s, CH), 4.00 (1H, s, CH), 4.64 (2H, m, CH, OH), 5.01–5.19 (3H, m, CH, OH), 7.70–7.76 (1H, m, Ph-H), 8.21–8.24 (2H, m, Ph-H), 8.58, 8.68 (1H, =CH), 8.68 (1H, s, Ph-H), 12.64, 12.82 (1H, NH). ^{13}C NMR (100 MHz, DMSO-d6): δ (ppm) 13.72, 22.75, 32.77, 33.62, 60.78, 61.08, 71.30, 74.25, 74.80, 82.26, 121.49, 122.87, 124.33, 130.70, 133.46, 136.67, 143.95, 148.61, 151.71, 153.62, 168.81. HRMS (ESI) for [M + H]$^+$: calcd 519.17688, found 519.17691.

Computational details

Density functional theory at B3LYP/6-31G (d,p) [24] theoretical level was used to optimize the geometries of all stationary points along the reaction paths. Frequency analysis calculations were carried out at the same level to classify the located stationary points as minima (no imaginary frequency) and transition states (only one imaginary frequency) and to obtain zero point energies (ZPES) and the thermodynamic correctional data. The B3LYP/6-31G (d,p) intrinsic reaction coordinate (IRC) pathways have also been computed of all the transition states to determine whether these transition states can connect the reactants, intermediates or products [25]. The single point energies of all the optimized structures were calculated at B3LYP/6-311G (d,p) level. All the energies listed in this paper were corrected by thermal corrections. The polarized continuum model (PCM) was used in Consistent Reaction Field (SCRF) with DMSO as solvent [26–28]. All of the quantum chemical calculations were performed using the Gaussian 09 program package [29]. All the geometrical coordination and single point energies of calculated structures were provided in Supporting Information.

## Results and discussion

NMR characterization

All the structures of synthesized compounds were determined by ^{1}H NMR, ^{13}C NMR and HRMS (Supporting Information Fig. S1–6). Among, the compound **1a** was selected as the model for structural characterization and its NMR spectra were presented in Fig. 1.

According to the ^{1}H NMR spectrum (Fig. 1a), signals at δ 1.01 (t, 3H), 1.73 (m, 2H), and 3.15 (m, 2H) were attributed to protons in propyl and peaks at δ 3.78 (t, 1H) and 3.97 (t, 1H) and 5.18 (d, 1H) due to the three hydrogens of hydroxyl, the assignments of the remained eight saturated protons signals attached at cyclopentane and ethylidene corresponding to the rest of peaks at up-field ranging from 2.05 to 5.09 ppm. Additionally, the four aromatic protons of phenyl were located at 6.83~7.81 ppm and the presence of the phenolic hydroxyl at 9.68 ppm. Finally, the hydrogen signals at 8.19~8.43 ppm and 12.36~12.54 ppm were regarded as belonging to C^{3}H and N′H, respectively.

To verified rationality of the assignment of the three protons at the lowest field in Fig. 1a, D$_2$O-exchange NMR experiment was performed and the spectrum was depicted in Fig. 1b, where both the signals at 9.68 ppm and 12.36~12.54 ppm were disappeared while the peaks at 8.19~8.43 ppm were remained, which illustrated that peaks at the disappeared location were correspondence with those of active hydrogens
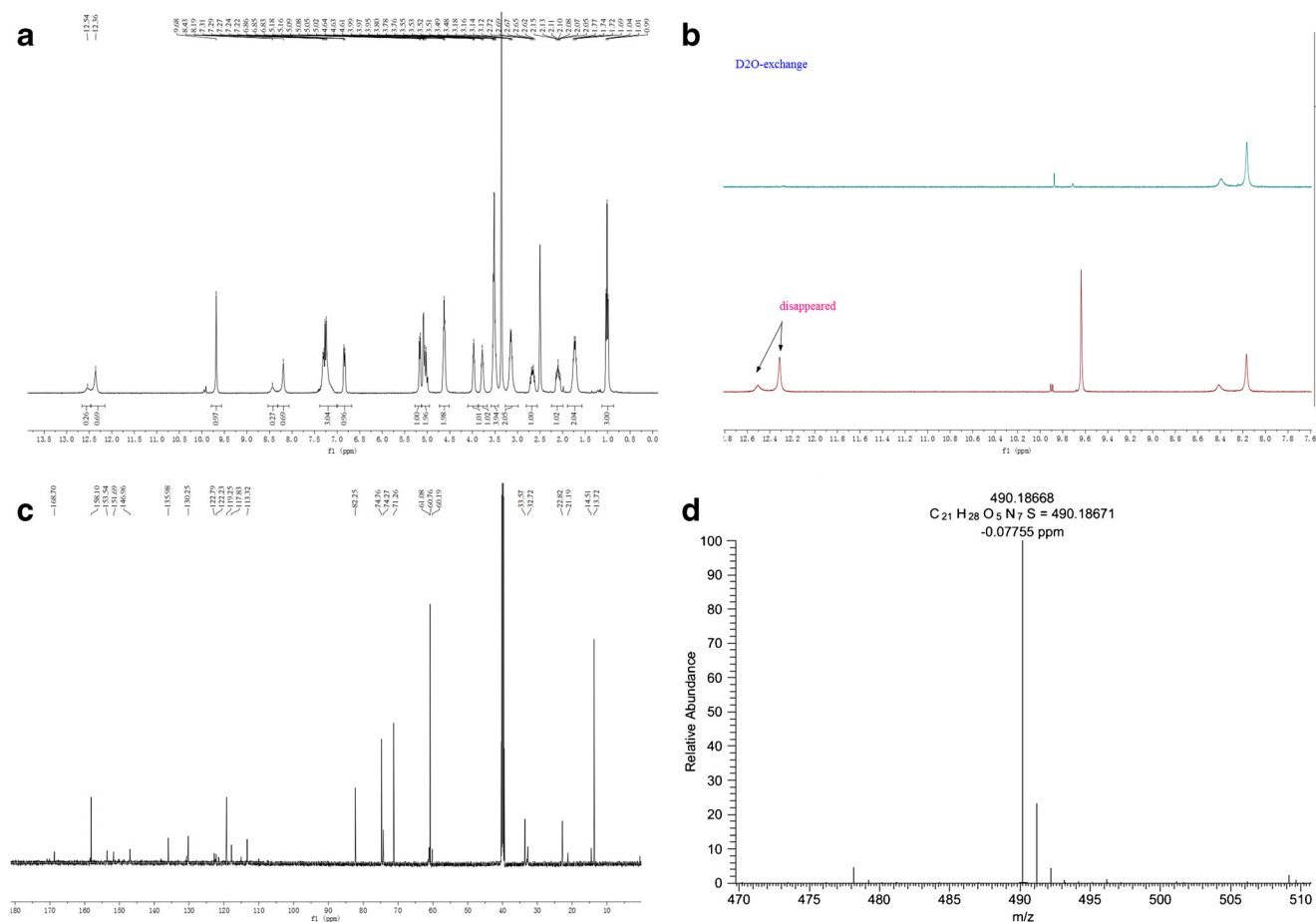
Fig. 1 Spectra of compound **1a**. **a** ^{1}H NMR. **b** D$_2$O-exchange. **c** ^{13}C NMR. **d** HRMS

that assigned as phenolic hydroxyl and NH and hence the remained one was the proton of C$^{3'}$H.

From the ^{13}C NMR spectrum (Fig. 1c), 21 carbon signals were observed. The first 10 peaks from 13.72 to 82.76 ppm were correlated with those sp^3 hybrid carbon atoms in the compound. The location of the phenylic and the olefinic carbon signals was found at 113.2~135.9 ppm and the distribution of carbon signals of the 8-azaadenine skeleton was located at 151.69~168.70 ppm. HRMS (ESI$^+$) of **1a** (Fig. 1d) shown a molecular ion peak at 490.18671 m/z, which was consistent with the calculated value (i.e., 490.18668 m/z) for **1a** [M]$^+$. Hereto, the structure of **1a** was established through these above data without controversy.

From Fig. 1a, one can readily noticed the duplications of proton signals at 8.19~8.43 ppm and 12.36~12.54 ppm, which were assigned as C$^{3'}$H and N$^{1'}$H, respectively. Particularly, the same consequence can be observed within all the titled compounds **1** (Fig. S1), of which the proton of C$^{3'}$H and N$^{1'}$H showed a broaden doublet peak. The relative chemical shifts were depicted in Table 1.

In general, this phenomenon was introduced by the presence of configurational isomers or conformational isomers in

molecular system. Contreras and colleagues' theoretically studies on the prototropic tautomerism of 8-azaadenine have shown that there are a number of tautomeric forms in the 8-azaadenine structure and among them, the 9H-azaade, 8H-azaade and 7H-azaade are more stable for their lower energy values [30]. Moreover, Wierzchowski's group speculated that 2-amino-8-azaadenine can exist in many different tautomeric forms and they predicted that the photo-induced proton transfer process of such compound is particularly useful for its application in fluorescence probe (Scheme 2a) [30]. On the other hand, previous studies about N-acylhydrazone (NAH) have shown that C = N double bond stereoisomers (E/Z) and

Table 1 ^{1}H NMR data of N$^{1'}$$\underline{H}$ and C$^{3'}$$\underline{H}$ protons for compounds **1**

| Compound no.	N$^{1'}$$\underline{H}$ (ppm)	C$^{3'}$$\underline{H}$ (ppm)
1a	12.36, 12.54	8.19, 8.43
1b	12.56, 12.71	8.22, 8.46
1c	12.76, 12.88	8.33, 8.60
1d	12.50, 12.64	8.32, 8.50
1e	12.64, 12.82	8.50, 8.68
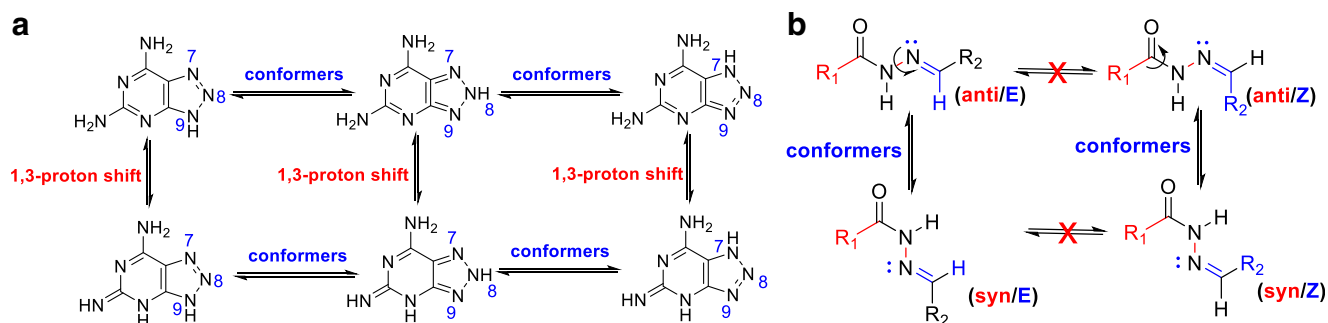
Scheme 2 **a** Structure and some possible tautomeric forms of 2,6-diamino-8-azapurine. **b** Stereoisomers and conformers of NAH

conformers (syn/anti) about the amide CO-NH bond may be observed (Scheme 2b), which depended on the assemblage of amide and imine functions. Furthermore, both the protons of benzyl and alkyl NAHs showed duplication signals, which was later proved to be induced by a mixture of two conformers of the samples in solution and the energy barrier of this conversion was calculated as about 17 kcal/mol via dynamic NMR experiments [31].

Inspiring by studies on the compounds 8-azapurines and hydrazones, we speculated that the isomers involved in the ¹H NMR spectrum of compounds **1** would incorporate two of the following structures displayed in Scheme 3. The compounds **1a** was also selected as the structural analysis model.

To find out what was the exactly dominated factor resulting in the occurrence of the doublet proton signals, primarily, the temperature-dependence ¹H NMR experiment was performed
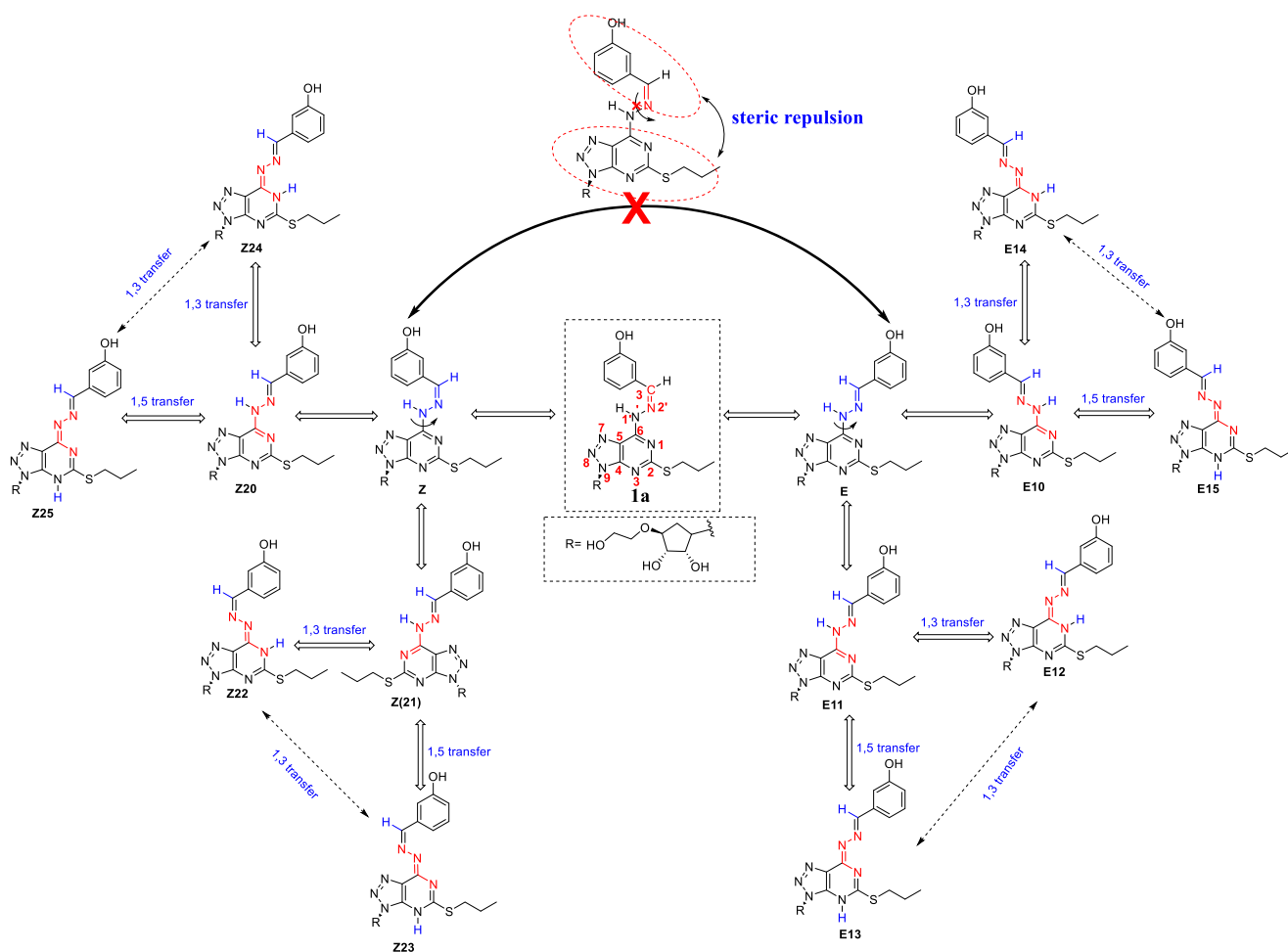
Scheme 3 Conceivable isomers of compound **1a**. (*Numbering in the scheme was just for simplicity and not obey the IUPAC rules*)
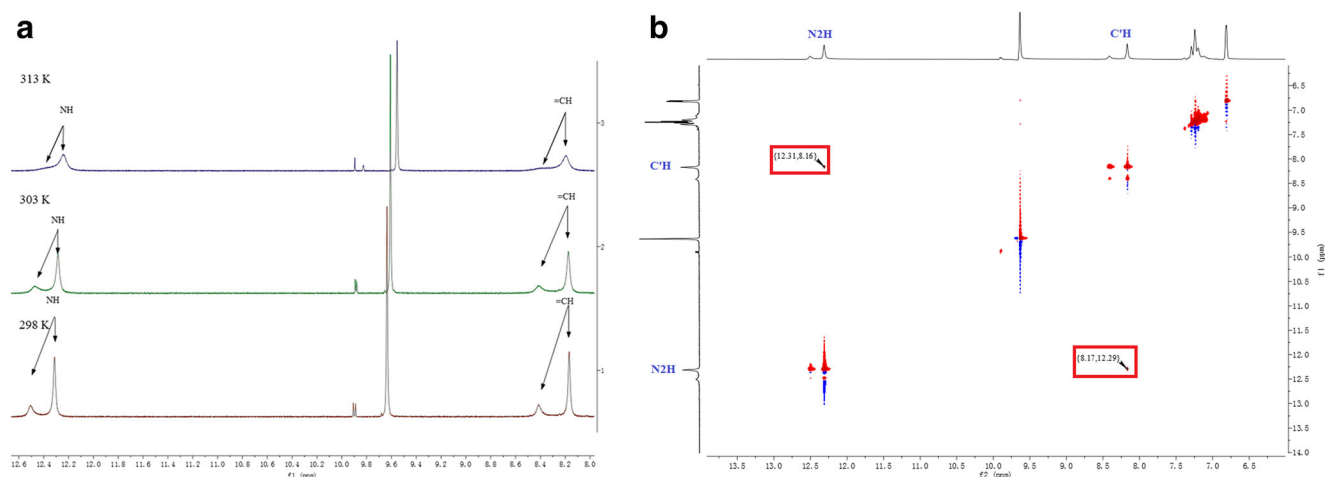
Fig. 2 Variable temperature ^{1}H NMR spectrum (a) and local amplified NOESY spectrum (b) of 1a.

using different temperature at 298 K, 303 K and 313 K, the spectrum as displayed in Fig. 2a. As can be seen from Fig. 2a, both the two groups of proton peaks of C$^{3'}$H and N$^{1'}$H were gradually coalesce at 303 K, and then merged into a singlet one with temperature increasing to 313 K, which implying that the duplication of these proton signals may be attributed to the presence of two isomers which interconvert slowly at ambient and the rate will be accelerated with temperature increasing.

With this result in hand, we then traced back to Scheme 3 for analyzing the possible configuration of 1a in solution. As shown in Scheme 3, a couple of stereoisomers (E/Z) would be observed with respect to C$^{3'}$ = N$^{2'}$ double bond, which were capable of forming configurational isomers E12~E15 and Z22~Z25 through 1,3-hydrogen transfer. Additionally, it was also readily accepted that the existence of conformational isomers of 1a in solution, generated by rotation of C^6-N$^{1'}$ single bond. Nonetheless, the rotation of N$^{1'}$-N$^{2'}$ bond was not taken into consideration for the steric repulsion effect between the arylhydrazone groups and the 8-azapurines moiety. In this case, combining with the result extracted from

variable temperature ^{1}H NMR spectra, we ruled out the possibility of simultaneous occurrence of E/Z on account of unable to interconvert each other of the two stereoisomers. Subsequently, we decided to proceed with 2D-NOESY experiments to access the relative stable configuration of 1a in solution (Fig. 2b).

According to Fig. 2b, besides the expected diagonal signals were observed, correlation at (8.17, 12.29 ppm), assigned to proton of C$^{3'}$H and hydrogen of N$^{1'}$H, was the straightforward evidence that the E configuration was adopted by 1a in solution. Hence, our follow-up theoretical studies were focused on investigating the E stereoisomers of 1 by using density functional theory.

Potential energy surface (PES) scan studies

In order to describe the conformational flexibility of the titled molecules, the energy profile as a function of N$^{2'}$-N$^{1'}$-C^6-N^1 torsion angle of compound 1a was shown in Fig. 3. All the geometrical parameters were simultaneously relaxed during the calculations while the variable was increased in steps of 10° from 180° to 360°. The torsional potential surface of the molecule was obtained by using the PM6 method [32]. From Fig. 3, two stable local minima cis-E (E11) and trans-E (E10) arising from aromatic hydrazone bond to N$^{1'}$ atom were obtained at 0° (360°) and 180°. Further geometrical optimization of these two structures was proceeded at B3LYP/6-31G (d,p) theoretical level. According to the DFT calculation the two conformers possessed similar energy, one was − 1973.960 Eh and the other was − 1973.958 Eh, the difference was just for 0.02 Eh. Moreover, from the calculations, the optimized structures of the two isomers were both coplanar between the aromatic hydrazone and the 8-azapurine ring. These resemblance illustrated that the two isomers may exist in solution may exist in solution simultaneously and therefore induce duplication of proton signal.
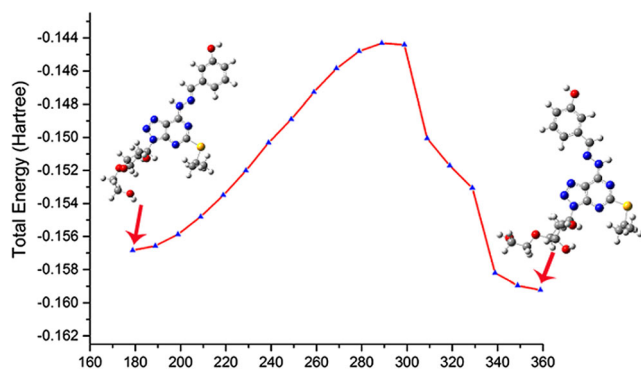
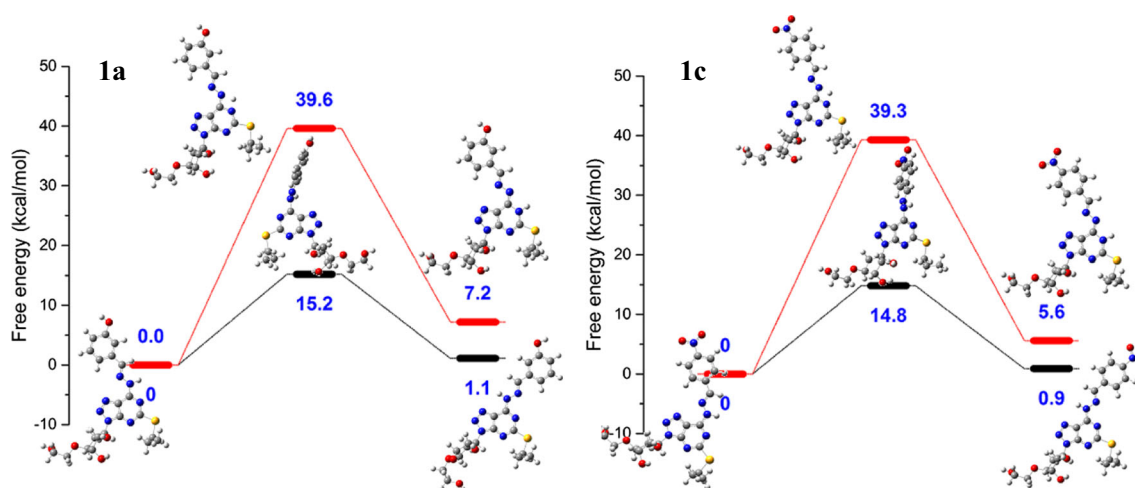Fig. 3 Potential energy surface scan for the selected dihedral angle of 1a (in DMSO)

Fig. 4 Energy profile for conformational isomerism and proton migration process of compounds **1a** and **1c**

Competition of proton migration and conformational isomerism process

Aiming at ascertaining the predominant factor between hydrogen transfer and interconversion causing reproduction of the proton peaks and interpreting the signals of $N^{1'}H$ and $C^{3'}H$ protons of **1c** at 298 K (Supporting Information Fig. S3) is similar to those of the other compounds in Scheme 1 at 313 K, we calculated the energy barriers for the two isomerization processes of compounds **1a** and **1c**, for instance. As shown in Fig. 4, the barriers for conformational isomerism of **1a** and **1c** were found be very closely, 15.2 and 14.8 kcal/mol, respectively, and far less than those for proton migration where the barriers were 39.6 and 39.3 kcal/mol, which indicated that the conformational isomerization was more favorable. Moreover, the energy barriers of **1c** were 0.4 kcal/mol smaller than **1a**, hinting the conformational isomerization of the former more accessible, which in good agreement with the ^1H NMR experiment result. Having known that reactions with a barrier of 21 kcal/mol or less will proceed readily at room temperature

[33], we concluded that the duplications of hydrogen peaks were attributed to conformational isomerism.

Additionally, variation tendency of the rate constants, k, for the **1a** and **1c** varied with temperature ranging from 298 K to 313 K were calculated via the transtion state theory (**TST**) and the resultant curves were shown in Fig. 5. Conspicuously, the rate constants of conformatioanal isomerism were 1.00E + 016 fold than hydrogen migration, which implied that the latter process can be considered as nonoccurrence in solution. In the case of conformatioanal isomerism process, the constant of **1c** increased from 15 s^{-1} to 50 s^{-1} with temperature changing from 298 K to 313 K. What is more, the rate of **1c** at 298 K was 50 s^{-1} greater than that of **1a** at the same temperature and 15 s^{-1} at 313 K; Furthermore, the differentials expanded to 150 s^{-1} when temperature of **1c** increased to 313 K. Undoubtedly, these results supported perfectly the conslusion that the conformatioanal isomerism was superior to proton migration and in completely agreement with experimental results that the duplications of hydrogen peaks for $N^{1'}H$ and $C^{3'}H$ in **1a** occurred at 298 K and then coalesce into a broaden
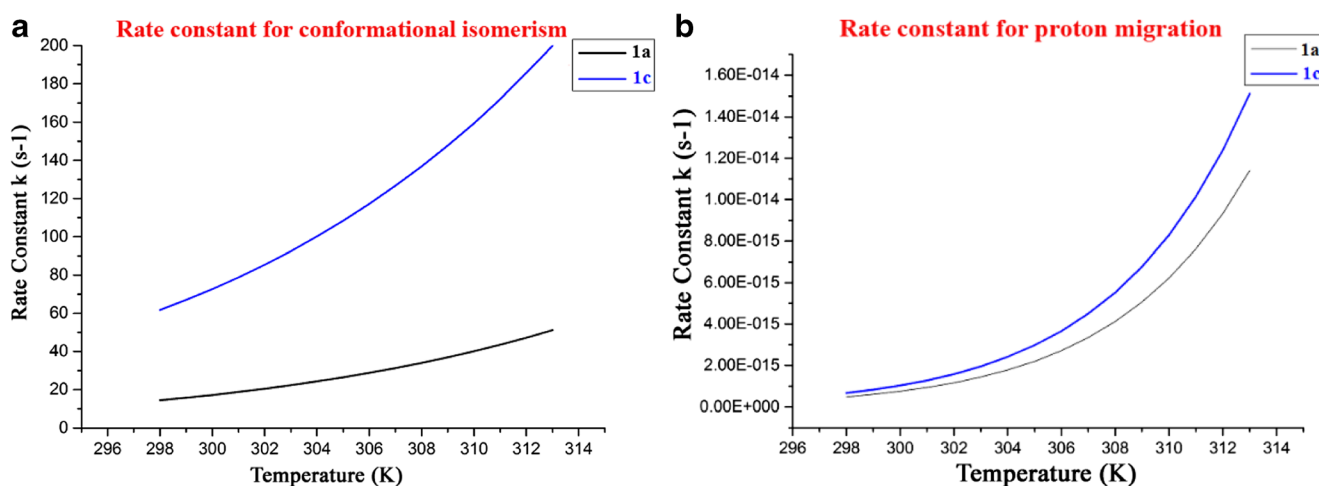

Fig. 5 The curves of rate constants varied with temperature for the conformatioanal isomerism (**a**) and proton migration (**b**) of **1a** and **1c**

one at 313 K and the shape of corresponging peaks of **1c** at 298 K were similar to those of **1a** at 313 K.

Conclusion

In this paper, we described the synthesis of 9-substituented-N^6-hydrazone-8-azapurines derivatives and characterized their structures via ^{1}H NMR, ^{13}C NMR and HRMS. The stereo structures of compounds **1** and the reason resulting in duplications of proton signals in ^{1}H NMR spectra of the synthesized compounds were analyzed through 2D-NOESY and variable temperature NMR techniques as well as DFT calculations at the level of B3LYP/6-311G (d,p)//B3LYP/6-31G (d,p). The 2D-NOESY spectrum showed that the **E** configuration of **1** was adopted in solution. The variable temperature NMR showed that the reproduction of hydrogen signals was induced by the presence of either tautomers resulting from proton transfer process or rotational isomers about the C^6-$N^{1'}$ bond. The DFT calculations showed that the resultant energy barriers of proton migration and conformational isomerism were about 40 kcal/mol and 15 kcal/mol, respectively. The rate constant for the conformational isomerism process was far less than that of proton transfer, $1.00E+01$ s^{-1} vs $1.00E$-015 s^{-1}. Combinding the experimental and theoretical calculating results, we thought that it was the conformers that introduced the duplication of proton signals of $C^{3'}$H and $N^{1'}$H.

Compliance with ethical standards

Conflict of interest   The authors declare that they have no conflicts of interest.

References

1. Montgomery JA, Shortnacy AT, Arnett G, Shannon W (1977) 2-Substituted derivatives of 9-. alpha.-D-arabinofuranosyladenine and 9-. alpha.-D-arabinofuranosyl-8-azaadenine. J Med Chem 20(3):401–404

2. Dvořáková H, Holý A, Masojidkova M, Votruba I, Balzarini J, Snoeck R, De Clercq E (1993) Synthesis and antiviral activity of acyclic nucleoside and nucleotide derivatives of 8-azaadenine. Collect Czechoslov Chem Commun 58(20):253–255

3. Massarelli I, Coi A, Pietra D, Nofal FA, Biagi G, Giorgi I, Leonardi M, Fiamingo F, Bianucci AM (2008) QSAR study on a novel series of 8-azaadenine analogues proposed as a 1 adenosine receptor antagonists. Eur J Med Chem 43(1):114–121

4. Chawla M, Credendino R, Oliva R, Cavallo L (2015) Structural and energetic impact of non-natural 7-deaza-8-azaadenine and its 7-substituted derivatives on H-bonding potential with uracil in RNA molecules. J Phys Chem B 119(41):12982–12989

5. Husted S, Van Giezen J (2009) Ticagrelor: the first reversibly binding oral P2Y12 receptor antagonist. Cardiovasc Ther 27(4):259–274

6. Havlicek L, Fuksova K, Krystof V, Orsag M, Vojtesek B, Strnad M (2005) 8-Azapurines as new inhibitors of cyclin-dependent kinases. Bioorg Med Chem 13(18):5399–5407

7. Santana L, Teijeira M, Uriarte E, Balzarini J, De Clercq E (1999) Synthesis and biological evaluation of 1,2-disubstituted carbonucleosides of 2-amino-6-substituted purine and 8-azapurine. Bioorg Med Chem Lett 18(4–5):1349–1352

8. Elliott RD, Montgomery JA (1977) Analogues of 8-azainosine. J Med Chem 20(1):116–120

9. Holý A, Dvořáková H, Jindřich J, Masojídková M, Buděšínský M, Balzarini J, Graciella Andrei A, Clercq ED (1996) Acyclic nucleotide analogs derived from 8-azapurines: synthesis and antiviral activity. J Med Chem 39(20):4073–4088

10. Vince R, Brownell J, Daluge S (1985) Carbocyclic analogs of xylofuranosylpurine nucleosides. Synthesis and antitumor activity. J Med Chem 16(9):1358–1360

11. Springthorpe B, Bailey A, Barton P, Birkinshaw TN, Bonnert RV, Brown RC, Chapman D, Dixon J, Guile SD, Humphries RG (2007) From ATP to AZD6140: the discovery of an orally active reversible P2Y receptor antagonist for the prevention of thrombosis. Bioorg Med Chem Lett 17(21):6013–6018

12. Wierzchowski J, Mędza G, Szabelski M, Stachelska-Wierzchowska A (2013) Properties of 2, 6-diamino-8-azapurine, a highly fluorescent purine analog and its N-alkyl derivatives: tautomerism and excited-state proton transfer reactions. J Photochem Photobiol A Chem 265:49–57

13. Wierzchowski J, Kulikowska E, Bzowska A, Holy A, Magnowska L, Shugar D (1999) Interactions of calf spleen purine nucleoside phosphorylase with antiviral acyclic nucleoside phosphonate inhibitors: kinetics and emission studies. Nucleosides & Nucleotides 18(4–5):875

14. Ward DC, Reich E, Stryer L (1972) Fluorescence studies of nucleotides and polynucleotides. I. Formycin, 2-aminopurine riboside, 2, 6-diaminopurine riboside, and their derivatives. J Biol Chem 247(12):4014–4020

15. Da Costa CP, Fedor MJ, Scott LG (2007) 8-Azaguanine reporter of purine ionization states in structured RNAs. J Am Chem Soc 129(11):3426–3432

16. Liu L, Cottrell JW, Scott LG, Fedor MJ (2009) Direct measurement of the ionization state of an essential guanine in the hairpin ribozyme. Nat Chem Biol 5(5):351

17. Viladoms J, Scott LG, Fedor MJ (2011) An active-site guanine participates in glmS ribozyme catalysis in its protonated state. J Am Chem Soc 133(45):18388

18. Mohamed TA, Hassan AE, Shaaban IA, Abuelela AM, Zoghaib WM (2017) Conformational stability, spectral analysis (infrared, Raman and NMR) and DFT calculations of 2-amino-5-(ethylthio)-1, 3, 4-thiadiazole. J Mol Struct 1130:434–441

19. Mitchell RH (2002) Conformational changes of 2, 11-dithia [3.3] metacyclophane. A new look using VT NMR and calculation. J Am Chem Soc 124(10):2352–2357

20. Witosińska A, Musielak B, Serda P, Owińska M, Rys B (2012) Conformation of eight-membered benzoannulated lactams by combined NMR and DFT studies. The Journal of organic chemistry 77(21):9784–9794

21. Santacruz-Juárez E, Höpfl H, Romero GHO, Castro A, Juaristi E, de Parrodi CA, Morales-Meza S, Sancheze M (2017) Synthesis and conformational analysis of novel tertiary amides derived from N-[(S)-α-phenylethyl]-1, 3-imidazolidine. Organic Chemistry (part v):89-99

22. Kozic J, Novák Z, Římal V, Profant V, Kuneš J, Vinšová J (2016) Conformations, equilibrium thermodynamics and rotational barriers of secondary thiobenzanilides. Tetrahedron 72(17):2072–2083

23. Tormena CF (2016) Conformational analysis of small molecules: NMR and quantum mechanics calculations. Prog Nucl Magn Reson Spectrosc 96:73–88

24. Stephens PJ, Devlin FJ, Chabalowski CF, Frisch MJ (1994) Ab initio calculation of vibrational absorption and circular dichroism spectra using density functional force fields. Chem Phys Lett 98(45):247–257

25. Gonzalez C, Schlegel HB (1989) An improved algorithm for reaction path following. J Chem Phys 90(90):2154–2161

26. Cossi M, Scalmani G, Rega N, Barone V (2002) New developments in the polarizable continuum model for quantum mechanical and classical calculations on molecules in solution. J Chem Phys 117(1):43–54

27. Miertuš S, Scrocco E, Tomasi J (1981) Electrostatic interaction of a solute with a continuum. A direct utilizaion of AB initio molecular potentials for the prevision of solvent effects. Chem Phys 55(1): 117–129

28. Miertus S, Tomasi J (1982) Approximate evaluations of the electrostatic free energy and internal energy changes in solution processes. Chem Phys 65(2):239–245

29. Frisch M, Trucks G, Schlegel HB, Scuseria G, Robb M, Cheeseman J, Scalmani G, Barone V, Mennucci B, Petersson G (2009) Gaussian 09, revision D. 01. Gaussian, Inc., Wallingford CT

30. Contreras JG, Madariaga ST, Alderete JB (1998) Theoretical study of the tautomerism of 8-azaadenine. J Phys Org Chem 11(6):392–396

31. Lopes AB, Miguez E, Kümmerle AE, Rumjanek VM, Fraga CAM, Barreiro EJ (2013) Characterization of amide bond conformers for a novel heterocyclic template of N-acylhydrazone derivatives. Molecules 18(10):11683–11704

32. Stewart JJ (2007) Optimization of parameters for semiempirical methods V: modification of NDDO approximations and application to 70 elements. J Mol Model 13(12):1173–1213

33. Young D (2004) Computational chemistry: a practical guide for applying techniques to real world problems. John Wiley & Sons, Hoboken